

NH₃ adsorption on anatase-TiO₂(101)

Cite as: J. Chem. Phys. **148**, 124704 (2018); <https://doi.org/10.1063/1.5021407>

Submitted: 04 January 2018 . Accepted: 16 February 2018 . Published Online: 23 March 2018

Stig Koust , Kræn C. Adamsen, Esben Leonhard Kolsbjerg , Zheshen Li , Bjørk Hammer , Stefan Wendt, and Jeppe V. Lauritsen 

COLLECTIONS

 This paper was selected as an Editor's Pick



[View Online](#)



[Export Citation](#)



[CrossMark](#)

ARTICLES YOU MAY BE INTERESTED IN

[Rotation and diffusion of naphthalene on Pt\(111\)](#)

The Journal of Chemical Physics **148**, 124703 (2018); <https://doi.org/10.1063/1.5017581>

[Perspective: A controversial benchmark system for water-oxide interfaces: H₂O/TiO₂\(110\)](#)

The Journal of Chemical Physics **147**, 040901 (2017); <https://doi.org/10.1063/1.4996116>

[Accelerating atomic structure search with cluster regularization](#)

The Journal of Chemical Physics **148**, 241734 (2018); <https://doi.org/10.1063/1.5023671>

NH₃ adsorption on anatase-TiO₂(101)

Stig Koust,¹ Kræn C. Adamsen,¹ Esben Leonhard Kolsbjerg,^{1,2} Zheshen Li,²
Bjørk Hammer,^{1,2} Stefan Wendt,¹ and Jeppe V. Lauritsen^{1,a)}

¹Interdisciplinary Nanoscience Center (*iNANO*), Aarhus University, DK-8000 Aarhus C, Denmark

²Department of Physics and Astronomy, Aarhus University, DK-8000 Aarhus C, Denmark

(Received 4 January 2018; accepted 16 February 2018; published online 23 March 2018)

The adsorption of ammonia on anatase TiO₂ is of fundamental importance for several catalytic applications of TiO₂ and for probing acid-base interactions. Utilizing high-resolution scanning tunneling microscopy (STM), synchrotron X-ray photoelectron spectroscopy, temperature-programmed desorption (TPD), and density functional theory (DFT), we identify the adsorption mode and quantify the adsorption strength on the anatase TiO₂(101) surface. It was found that ammonia adsorbs non-dissociatively as NH₃ on regular five-fold coordinated titanium surface sites (5f-Ti) with an estimated exothermic adsorption energy of 1.2 eV for an isolated ammonia molecule. For higher adsorbate coverages, the adsorption energy progressively shifts to smaller values, due to repulsive intermolecular interactions. The repulsive adsorbate-adsorbate interactions are quantified using DFT and autocorrelation analysis of STM images, which both showed a repulsive energy of ~50 meV for nearest neighbor sites and a lowering in binding energy for an ammonia molecule in a full monolayer of 0.28 eV, which is in agreement with TPD spectra. Published by AIP Publishing. <https://doi.org/10.1063/1.5021407>

I. INTRODUCTION

Titanium dioxide (TiO₂) is used in many applications such as Grätzel solar cells,¹ heterogeneous catalysis,^{2–5} and photocatalysis.^{6,7} Among the main polymorphs of TiO₂, rutile, anatase, and brookite, only the former two are used in technical applications.^{2,7} Whereas rutile has traditionally been the most studied polymorph in the surface science literature,⁷ anatase has bulk and surface properties that make this polymorph the most relevant for, e.g., photocatalytic and heterogeneously catalysed reactions.

For this reason, the most stable of the anatase facets, the TiO₂(101) surface [a-TiO₂(101)], has been the subject of numerous studies addressing the adsorption of small molecules, such as CO,^{8,9} H₂O,^{10–12} O₂,¹³ and acetic acid.¹⁴ These studies have shown a rather complex behavior of these simple molecules, although their adsorption seems to be less dominated by bulk and surface defects than for rutile TiO₂. Here we focus on the fundamental interaction of NH₃ with a-TiO₂(101). The NH₃ adsorption on a-TiO₂(101) is highly important, insofar as adsorption studies of NH₃ with a-TiO₂ have been used to probe Lewis acid-base interactions with anatase powders.¹⁵ In addition, the NH₃/anatase TiO₂ system is of importance in the selective catalytic reduction (SCR) of NO with NH₃ using submonolayer vanadium oxides on a-TiO₂^{2,16} or for titania-based catalysts for the removal of NH₃ pollution from air and water.^{17,18}

Studies addressing the NH₃ adsorption on the rutile polymorph, r-TiO₂(110), have employed scanning tunneling microscopy (STM),¹⁹ temperature programmed desorption (TPD),^{20,21} X-ray photoemission spectroscopy (XPS),^{21–23}

and theoretical calculations^{15,24,25} to conclude that ammonia adsorbs molecularly on five-fold coordinated titanium (5f-Ti) surface sites and desorbs again without dissociation. The desorption energy was found to be coverage-dependent and decrease from ~1.0–1.3 eV^{20,21} at low NH₃ coverage to ~0.6 eV at full monolayer coverage. This is reasoned by repulsive NH₃–NH₃ interactions which cause the ammonia to occupy every second 5f-Ti surface site.^{19,22,23,26} On r-TiO₂(110), a full monolayer is therefore considered in some studies to be achieved by the occupation of half the available 5f-Ti sites.^{19,22} However, Kim *et al.*²⁰ reported by using TPD that a full NH₃ monolayer on rutile TiO₂ (110) corresponds to occupation of all 5f-Ti sites.

The present study combines STM, XPS, TPD, and density functional theory (DFT) to reveal the adsorption mode, intermolecular interactions, and desorption of NH₃ on a-TiO₂(101). Our STM and DFT results reveal the preferential adsorption site to be on 5f-Ti surface sites of a-TiO₂(101). We conclude that NH₃ adsorbs and desorbs molecularly based on XPS and TPD. In line with comparable studies of NH₃ monolayers on r-TiO₂(110), we find that repulsive interactions between neighboring NH₃ molecules influence binding energies, reflected by an observed intermediate (2 × 1) superstructure. However a full NH₃ monolayer is considered as occupation of all 5f-Ti-sites.

II. EXPERIMENTAL

The STM and TPD experiments were performed in an ultra-high vacuum chamber (SPECS) with a base pressure below 1×10^{-10} mbar, equipped with a commercial Aarhus-type STM (Aarhus-150, SPECS) that allows for cooling to liquid nitrogen temperatures. Tungsten (W) STM tips prepared

^{a)}Electronic mail: jvang@inano.au.dk

by electrochemical etching were used for imaging. Typical scanning parameters were 1000–1400 mV and 0.1–0.2 nA. All TPD spectra were acquired using a quadrupole mass spectrometer (HIDEN). The XPS experiments were carried out at the ASTRID2 synchrotron source at the Institute for Storage Ring Facilities (ISA) at Aarhus University on the AU-MatLine beamline.²⁷ The beamline is equipped with a SX-700 monochromator and SCIENTA SES200 electron energy analyzer running with a pass energy of 75 eV, curved analyzer slit of 0.8 mm, and a beamline monochromator slit width of 60 μ m. The base pressure was around 5×10^{-10} mbar. The N1s core level was collected using a photon energy of 480 eV.

Natural anatase single crystals (SurfaceNet) were prepared by preparation cycles of sputtering (Ar^+ , 1.5 kV, 298 K), O_2 annealing (1×10^{-8} mbar, 820–950 K), and subsequent sputtering and vacuum-annealing (820–950 K). The temperature of the sample is measured by a K-type thermocouple spot-welded onto the sample holder close to the sample. NH_3 was dosed on to the anatase $\text{TiO}_2(101)$ surface through a leak valve by means of a directional doser. This was done to minimize ammonia contaminants in the residual gas and thereby minimize re-adsorption onto the surface after the initial exposure. Typical exposures for submonolayer coverage of NH_3 were 5×10^{-10} mbar for 1–2 s. The coverage is given in ML, with 1 ML defined as one NH_3 molecule per Ti surface atom in the $\text{a-TiO}_2(101)$ surface, i.e., 9.7×10^{14} NH_3 molecules per cm^2 .

For constructing, manipulating, and optimizing the atomistic systems, the ASE²⁸ package was used in combination with the GPAW²⁹ density functional theory (DFT) code. We use the grid-based mode of GPAW with a spacing of at least 0.1771 Å sampling $4 \times 4 \times 1$ K-points of the Brillouin zone. To mimic the experimental crystal, we employ a 4-layer TiO_2 (101) anatase slab spanning 1×2 surface unit cells, resulting in a total stoichiometry of $\text{Ti}_{24}\text{O}_{48}$. We use the optB88-vdW functional with optimized lattice parameters of $a = b = 3.82$ Å and $c = 9.61$ Å with periodic boundary conditions parallel to the slab surface with at least 6 Å of vacuum from any atom to the non-periodic cell boundaries. The bottom layer was held frozen, and systems were considered converged when no force on any atom exceeded 0.025 eV/Å.

III. RESULTS AND DISCUSSION

Figure 1 shows STM images following NH_3 exposure at room temperature (RT). The $\text{a-TiO}_2(101)$ surface exhibits large trapezoidal islands separated by monoatomic steps typical for this surface.³⁰ As we expose the clean $\text{a-TiO}_2(101)$ surface to 0.05 ML ammonia, bright protrusions appear in the STM image reflecting adsorption at room temperature. The ammonia-related protrusions reside homogeneously across the terraces [Fig. 1(a)]. The protrusions appear to have little affinity for binding at step edges, and no apparent agglomeration of molecules was observed. In order to illustrate local structural information of the adsorbed ammonia, we present a high-resolution (6 nm × 6 nm) STM image in Fig. 1(b). The superimposed lattice points (red circles) are attributed to protruding two-fold coordinated O atoms (2f-O) on $\text{a-TiO}_2(101)$. The bright features associated with ammonia (blue circles) are observed to bind in between the surface lattice rows running in the [010] direction in a position which is slightly displaced toward one of the rows. The fivefold coordinated Ti atoms (5f-Ti) terminating the $\text{a-TiO}_2(101)$ surface (gray) are also illustrated in the STM image, and their position coincides with the adsorption site of ammonia. Thus, the STM data suggest that ammonia binds to the $\text{a-TiO}_2(101)$ surface on top of the 5f-Ti surface sites. In agreement, we find from DFT that ammonia is predicted to adsorb molecularly without dissociation with an exothermic adsorption energy of 1.20 eV. The DFT-calculated adsorption site of isolated NH_3 molecules on a stoichiometric $\text{a-TiO}_2(101)$ is indeed found to be on 5f-Ti, as illustrated in Fig. 1(c). The ammonia is found off-centered between 2f-O rows running in the [010] direction.

XPS data were collected in order to verify the non-dissociative binding of molecular ammonia to $\text{a-TiO}_2(101)$. XPS allows for easy distinction between various amines as the shift in N1s binding energy between NH_2 , NH_3 , and NH_4 is in the order of 1.5 eV.³¹ We exposed the a-TiO_2 (101) surface to more than a monolayer of ammonia at 118 K and collected the N1s core level spectra (Fig. 2). This was followed by stepwise heating at elevated temperatures for 5 min until the N1s signal vanished. The XPS data were collected at ~120 K throughout the series. The N1s peak position is found at 400.9 eV for all temperatures and can be fitted with a

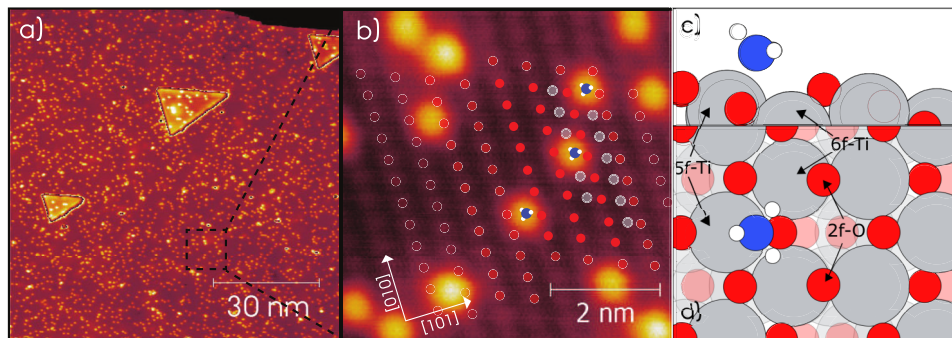


FIG. 1. (a) STM image (120 nm × 120 nm) of 0.05 ML NH_3 adsorbed on anatase- $\text{TiO}_2(101)$, imaged at RT. (b) Atom-resolved STM (6 nm × 6 nm) image at room temperature, showing the NH_3 adsorption site. Rows of surface lattice points [2f-O (red) and 5f-Ti (gray)] are superimposed. NH_3 (blue/white) molecules reside between rows, on top of the 5f-Ti sublattice. [(c) and (d)] DFT-predicted NH_3 adsorption site on 5f-Ti. (c) shows a side view of adsorbed ammonia and (d) shows a top view.

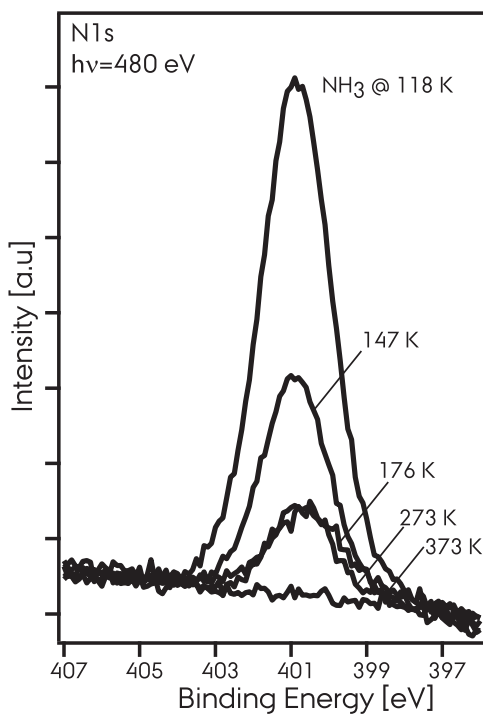


FIG. 2. N1s XPS spectra ($h\nu = 480$ eV, data collection at 110 K) of NH_3 adsorbed on anatase TiO_2 (101) (at 110 K) after heating in the range 118 K–373 K.

single peak with FWHM of 1.8 eV, indicating that only a single nitrogen species is present on the surface at all temperatures. This binding energy for nitrogen corresponds to molecularly adsorbed NH_3 bound to a Lewis acid center, thus a $\text{NH}_3\text{--Ti}$ bond.^{21,22,31,32} A dative bond with a Lewis acid center is formed by donation of a free electron pair from nitrogen.³¹ The N1s intensity decreases upon heating to 147 K and further at 176 K but then stays constant up to 273 K. Complete desorption of NH_3 was found after heating up to 373 K. This evolution of the N1s intensity suggests that multilayers of NH_3 accommodate the surface at the lowest temperature. The multilayer desorbs for temperatures around 176 K, where a stable monolayer is left on the surface, which is stable up to temperatures at 373 K. This is corroborated by TPD studies of ammonia desorption, which furthermore indicates considerable adsorbate-adsorbate interactions. In the TPD experiment, NH_3 was adsorbed on the $\alpha\text{-TiO}_2$ (101) surface at ~ 100 K in various coverages, followed by a linear temperature ramp rate (β) of 0.5 K s^{-1} to 600 K. The corresponding desorption spectra ($m/z = 17$) are presented in Fig. 3. The coverage is estimated by relating the integrated areas for the different spectra to the spectrum where multilayers start forming. At the lowest coverage, a single high temperature desorption peak around 410 K is observed. For higher coverages, the leading edge shifts progressively toward lower temperature, whereas the trailing edge stays constant, resulting in a broadening of the desorption peak. The desorption peak maximum shifts from 410 K (lowest coverage) to 327 K (full monolayer) in the submonolayer regime. For coverages above a monolayer, we observe a multilayer desorption peak forming around 180 K. The decrease in temperature of desorption peak maximum (T_m) for increasing NH_3 coverage indicates a strongly coverage-dependent

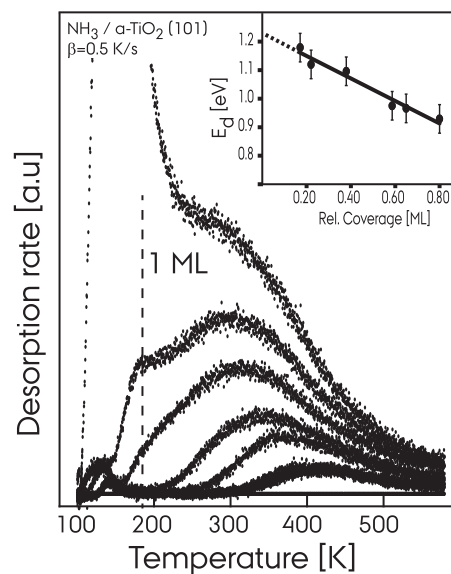


FIG. 3. TPD spectra of NH_3 ($m/z = 17$) adsorbed on anatase- TiO_2 (101) for various coverages (0.2–1.8 ML). Inset shows redheat analysis of TPD spectra, i.e., showing the change in binding energy as a function of coverage (peak area).

desorption energy (E_d), which can be calculated on the basis of T_m . We note that this method is valid strictly for first-order desorption.³³ This is fulfilled for non-dissociative adsorption,²⁰ despite the shift of maximum desorption to lower temperature with increasing coverages, which is otherwise typically related to second-order desorption.³⁴ E_d is calculated iteratively from the following equation:

$$E_d = k_b T_m \ln \left[\frac{k_b T_m^2 \nu}{E_d \beta} \right], \quad (1)$$

where the pre-exponential factor (ν) is calculated as in Ref. 34 to be $1.8 \times 10^{13} \text{ s}^{-1}$, which coincides with previously published values.^{20,33,34} E_d as a function of coverage in the submonolayer regime is presented in the inset in Fig. 3. We observed a shift from 1.18 eV to 0.93 eV for increasing coverage. Extrapolating to the zero coverage limit yields E_d of a single ammonia molecule on $\alpha\text{-TiO}_2$ (101) to be 1.23 ± 0.1 eV, which is in excellent agreement with theory (1.2 eV). In this limit $\text{NH}_3\text{--NH}_3$ interactions can be neglected; thus only the $\text{NH}_3\text{--TiO}_2$ interaction is determining E_d for an isolated NH_3 molecule.

The TPD spectra are also in accordance with the desorption trend observed in the XPS spectra (Fig. 2), as multilayer coverages were seen to desorb in the temperature range below 176 K, whereas a complete desorption occurred at temperatures higher than 276 K. The strong coverage-dependent desorption energy is attributed to the repulsion between ammonia molecules.^{20,21} A small tail is seen at the trailing edge at around 450 K; this is presumably caused by ammonia adsorption in vicinity of defects (subsurface donors), as only small affinity for adsorption at step edges is observed.

The repulsive interaction between NH_3 molecules was further quantified by analyzing the autocorrelation function of the ammonia positions (Fig. 4) from our STM data (Fig. 5) and comparing with DFT values for adsorption with a second NH_3

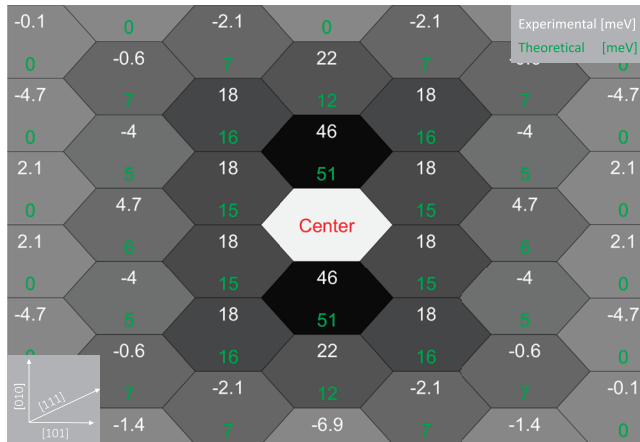


FIG. 4. Result of the autocorrelation function analysis, showing the obtained repulsion energies in meV. Experimental in white and theoretical in green. Each hexagon represents a neighboring Ti-5f site to the center. The gray color scale of each tile represents its likelihood of occupation (p_n). Black: less probable, i.e., high repulsion energy, white: very probable, gray: no effect.

molecule within the supercell modeling the a-TiO₂(101) surface. By marking the positions of adsorbed NH₃ molecules in an automated process and assigning them to an adsorption site, the probabilities of occupations are calculated. This is visualized in Fig. 4, by the gray scale colormap. The experimental repulsion energy (E_{rep}) is extracted by⁸

$$E_{rep} = -kT \ln \left(\frac{p_n}{p_{av}} \right), \quad (2)$$

where p_n denotes the probability for occupying neighboring site obtained directly from our autocorrelation analysis and p_{av} denotes the average probability for a random 5f-Ti site (coverage). Assuming the occupation of sites follow a Boltzmann distribution, the repulsion energy can be extracted. The experimentally extracted repulsion energies are displayed in Fig. 4 in white, on a grid reflecting the lattice of NH₃ adsorption sites. The values are shown together with the change in theoretical (DFT) adsorption energy with NH₃ on the neighboring sites in green. Very good agreement between theory and experimental acquired values are observed. In general, the nearest neighbor sites along the [010] are considerably less favorable than next-nearest neighbor adsorption sites and other sites further away. The nearest neighbor sites show repulsion energies of ~50 meV, next-nearest neighbor sites show ~20 meV, and sites further away show repulsion energy close to zero which reflects randomly distributed molecules. These results are also in good qualitative agreement with the observed NH₃ positions observed in Fig. 5 as nearest neighbor adsorption

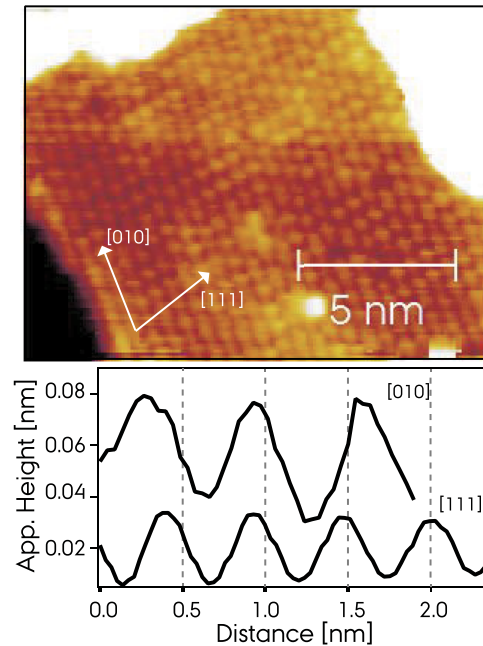


FIG. 6. STM (15 nm × 11 nm) image of NH₃ adsorbed on anatase-TiO₂(101) at 110 K. Inset: Linescan along the [111] and [010] directions, respectively.

sites are rarely observed. By increasing the ammonia coverage (Fig. 5), the STM images show local patterns of double lattice distance along the [010] directions (Fig. 5). Patterns along [111] direction are also observed (Fig. 5). We found that at even higher coverages, STM imaging becomes troublesome at room temperature, because of rapidly diffusing ammonia molecules. This can be circumvented at lower imaging temperatures (~100 K), where a static ordered overlayer structure can be imaged (Fig. 6). The overlayer consists of patches of adsorbed ammonia separated by ~5.5 Å formed in the [111] direction upon dosage and a longer distance of 7.8 Å along [010] directions. The intermolecular distances in the ordered areas (7.8 Å × 5.6 Å) coincide with a (2 × 1) symmetry with the underlying 5f-Ti surface atoms, i.e., a NH₃-(2 × 1)-TiO₂ overlayer. No STM images were obtained when further increasing the NH₃ coverage; thus, only TPD and XPS measurements are present for full monolayer coverages.

By adding all the obtained experimental or theoretical repulsion energies (Fig. 4), the adsorption energy per ammonia molecule for a full monolayer (all 5f-Ti sites occupied) is estimated to be 0.28 eV less than for the low coverage situation. The shift in energy between the low coverage adsorption and a full monolayer is in agreement with desorption features in the

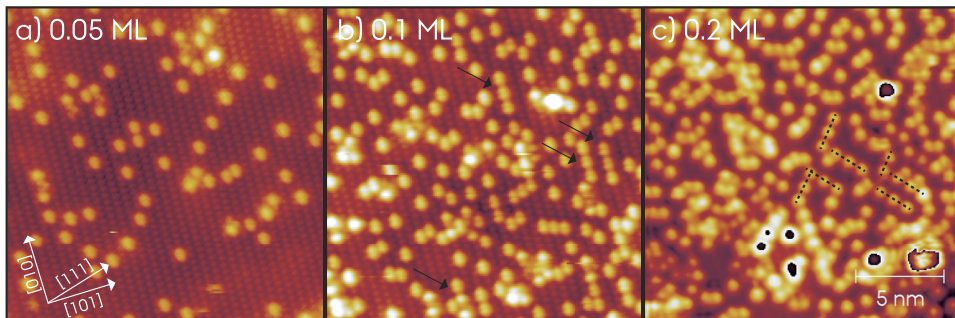


FIG. 5. STM (18 nm × 18 nm) image of NH₃ adsorbed on anatase-TiO₂(101) at RT at various coverages. (a) 0.05 ML, (b) 0.1 ML, (c) 0.2 ML.

TPD, where a shift of 0.28 eV is seen in Fig. 3, inset, i.e., NH₃ in a full monolayer is destabilized by this energy compared to a single NH₃. Compared with the NH₃/rutile-TiO₂(110) system,^{20,21} the adsorption of NH₃ on TiO₂(101) is very similar. The NH₃ adsorption sites are on 5f-Ti atoms on both surfaces. For a-TiO₂(101), we detect a significant NH₃-NH₃ repulsion reflected by a coverage-dependent desorption energy, but the effect is weaker than on rutile-TiO₂(110), which can be explained by a larger 5f-Ti spacing in anatase (101) compared to rutile (110) TiO₂ (3.78 Å and 2.96 Å, respectively).

IV. CONCLUSION

In summary, by high-resolution STM combined with XPS, TPD, and DFT, we find that NH₃ adsorbs molecularly on anatase TiO₂ (101). Specifically, when NH₃ was deposited at sub-monolayer coverage at room temperature, we found an affinity for NH₃ to reside at 5f-Ti atom sites. The theoretical adsorption energy (DFT) was calculated to be 1.20 eV and measured by TPD analysis to be 1.23 eV. Our XPS and TPD data indicated that NH₃ did not undergo dissociation at elevated temperatures and desorbed molecularly. Upon increasing the coverage, the NH₃ adsorption energy was significantly lowered by 0.28 eV because of dipole-dipole repulsive interactions, confirmed by TPD and autocorrelation analysis of STM images. In addition, the strong interaction between NH₃ resulted in a preference for occupying next-nearest 5f-Ti neighbor sites along the [010] direction, whereas NH₃ molecules occupying adjacent nearest neighbor sites in the [101] direction was seldom, and a repulsion energy of ~50 meV was found for this site from DFT and autocorrelation analysis of low NH₃ coverage STM images. Furthermore, an intermediate (2 × 1) overlay NH₃ adsorbate structure was observed at low temperature as a result of the intermolecular interaction.

ACKNOWLEDGMENTS

This work was partly funded by the Innovation Fund Denmark (IFD) under File Nos. 12-132681 (Cat-C) and 6151-00008B (ProNOx), VILLUM FONDEN (Investigator grant, Project No. 16562), and Danish Research Councils (No. 0602-02566B). We gratefully acknowledge support from Haldor Topsøe A/S. We acknowledge beamtime received at ASTRID2 on the MatLine beamline.

¹M. Grätzel, *J. Photochem. Photobiol., C* **4**, 145 (2003).

²G. Busca, L. Lietti, G. Ramis, and F. Berti, *Appl. Catal., B* **18**, 1 (1998).

³I. E. Wachs, *Dalton Trans.* **42**, 11762 (2013).

⁴L. Artiglia, S. Agnoli, and G. Granozzi, *Coord. Chem. Rev.* **301**, 106 (2015).

⁵N. Y. Topsøe, H. Topsøe, and J. Dumesic, *J. Catal.* **151**, 226 (1995).

⁶B. M. Weckhuysen and D. E. Keller, *Catal. Today* **78**, 25 (2003).

⁷U. Diebold, *Surf. Sci. Rep.* **48**, 53 (2003).

⁸M. Setvin, M. Buchholz, W. Hou, C. Zhang, B. Stöger, J. Hulva, T. Simschitz, X. Shi, J. Pavalec, G. S. Parkinson, M. Xu, Y. Wang, M. Schmid, C. Wöll, A. Selloni, and U. Diebold, *J. Phys. Chem. C* **119**, 21044 (2015).

⁹M. Setvin, B. Daniel, U. Aschauer, W. Hou, Y.-F. Li, M. Schmid, A. Selloni, and U. Diebold, *Phys. Chem. Chem. Phys.* **16**, 21524 (2014).

¹⁰C. Dette, M. A. Pérez-Osorio, S. Mangel, F. Giustino, S. J. Jung, and K. Kern, *J. Phys. Chem. C* **121**, 1182 (2017).

¹¹Y. He, A. Tilocca, O. Dulub, A. Selloni, and U. Diebold, *Nat. Mater.* **8**, 585 (2009).

¹²G. S. Herman, Z. Dohnalek, N. Ruzicka, and U. Diebold, *J. Phys. Chem. B* **107**, 2788 (2003).

¹³M. Setvin, M. Wagner, M. Schmid, G. S. Parkinson, and U. Diebold, *Chem. Soc. Rev.* **46**, 1772 (2017).

¹⁴D. C. Grinter, M. Nicotra, and G. Thornton, *J. Phys. Chem. C* **116**, 11643 (2012).

¹⁵A. Markovits, J. Ahdjoudj, and C. Minot, *Surf. Sci.* **365**, 649 (1996).

¹⁶I. E. Wachs, G. Deo, B. M. Weckhuysen, A. Andreini, M. Vuurman, M. de Boer, and M. D. Amiridis, *J. Catal.* **161**, 211–221 (1996).

¹⁷J. Lee, H. Park, and W. Choi, *Environ. Sci. Technol.* **36**, 5462 (2002).

¹⁸S. Yamazoe, T. Okumura, Y. Hitomi, T. Shishido, and T. Tanaka, *J. Phys. Chem. C* **111**, 11077 (2007).

¹⁹C. L. Pang, A. Sasahara, and H. Onishi, *Nanotechnology* **18**, 44003 (2007).

²⁰B. Kim, Z. Li, B. D. Kay, Z. Dohnalek, and Y. K. Kim, *Phys. Chem. Chem. Phys.* **14**, 15060 (2012).

²¹E. Farfan-Arribas and R. J. Madix, *J. Phys. Chem. B* **107**, 3225 (2003).

²²U. Diebold and T. E. Madey, *J. Vac. Sci. Technol., A* **10**, 2327 (1992).

²³W. K. Siu, R. A. Bartynski, and S. L. Hulbert, *J. Chem. Phys.* **113**, 10697 (2000).

²⁴D. Cheng, J. Lan, D. Cao, and W. Wang, *Appl. Catal., B* **106**, 510 (2011).

²⁵J. G. Chang, S. P. Ju, C. S. Chang, and H. T. Chen, *J. Phys. Chem. C* **113**, 6663 (2009).

²⁶J. N. Wilson and H. Idriss, *Langmuir* **20**, 10956 (2004).

²⁷Z. Li, <http://www.isa.au.dk/facilities/astrid2/beamlines/AU-Matline/AU-Matline.asp>.

²⁸A. Larsen, J. Mortensen, J. Blomqvist, I. Castelli, R. Christensen, M. Dulak, J. Friis, M. Groves, B. Hammer, C. Hargus, E. Hermes, P. Jennings, P. B. Jensen, J. Kermode, J. Kitchin, E. L. Kolsbjerg, J. Kubal, K. Kaasbjerg, S. Lysgaard, J. B. Maronsson, T. Maxson, T. Olsen, L. Pastewka, A. Peterson, C. Rostgaard, J. Schiøtz, O. Schütt, M. Strange, K. S. Thygesen, T. Vegge, L. Wilhelmsen, M. Walter, Z. Zeng, and K. W. Jacobsen, *J. Phys.: Condens. Matter* **29**, 273002 (2017).

²⁹J. Enkovaara, C. Rostgaard, J. J. Mortensen, J. Chen, M. Dułak, L. Ferrighi, J. Gavnholt, C. Glinsvad, V. Haikola, H. A. Hansen, H. H. Kristoffersen, M. Kuisma, A. H. Larsen, L. Lehtovaara, M. Ljungberg, O. Lopez-Acevedo, P. G. Moses, J. Ojanen, T. Olsen, V. Petzold, N. A. Romero, J. Stausholm-Møller, M. Strange, G. A. Tritsaris, M. Vanin, M. Walter, B. Hammer, H. Häkkinen, G. K. H. Madsen, R. M. Nieminen, J. K. Nørskov, M. Puska, T. T. Rantala, J. Schiøtz, K. S. Thygesen, and K. W. Jacobsen, *J. Phys.: Condens. Matter* **22**, 253202 (2010).

³⁰W. Hebenstreit, N. Ruzicka, G. S. Herman, Y. Gao, and U. Diebold, *Phys. Rev. B* **62**, R16334 (2000).

³¹C. Guimon, A. Gervasini, and A. Auoux, *J. Phys. Chem. B* **105**, 10316 (2001).

³²J. Keränen, C. Guimon, E. Iiskola, A. Auoux, and L. Niinistö, *Catal. Today* **78**, 149 (2003).

³³A. M. de Jong and J. W. Niemantsverdriet, *Surf. Sci.* **233**, 355 (1990).

³⁴I. Chorkendorff and J. W. Niemantsverdriet, *Concepts of Modern Catalysis and Kinetics* (Wiley, 2003).